Article

The Design of a Tracking Controller for Flexible Ball Screw Feed System Based on Integral Sliding Mode Control with a Generalized Extended State Observer

Muzhi Zhu [1,*], **Dafei Bao** [2] **and Xingrong Huang** [1]

1   School of Mechanical Engineering, Nanjing Institute of Technology, Nanjing 211167, China; hxr0146@163.com
2   Jiangsu Mingzhu Testing Machinery Co., Ltd., Yangzhou 225000, China; baodafei2009@163.com
*   Correspondence: zhumuzhi1021@126.com

Abstract: This article proposes a servo control strategy for compensating matched and mismatched perturbations in flexible ball screw feed systems to improve their tracking performance. The perturbations that satisfy or dissatisfy the matching conditions include external disturbances, parameter uncertainties, and unmodeled dynamics. The flexible ball screw feed model includes both a rigid body and first-order axial structural dynamics. A generalized extended state observer is adopted to observe the matched and mismatched perturbations and various state variables of the system, and an improved integral sliding mode controller is proposed that can simultaneously compensate for the perturbations of the system that satisfy and dissatisfy the matching conditions. In addition, vibration compensation is designed for first-order axial vibration of the system to develop a controller that can quickly and accurately track the ideal reference trajectory, suppress system structural vibrations, and be robust to time-varying uncertainties and external disturbances. Finally, the tracking performance, anti-interference performance, and vibration suppression performance of the designed controller are verified via simulation and comparative experiments.

Keywords: ball screw feed system; matched and mismatched perturbations; generalized extended state observer; integral sliding mode controller; vibration compensation

1. Introduction

In industrial production, cutting through machine tools is the most common way of part production and manufacturing. The ball screw has high rigidity and transmission efficiency and has been widely used in the feed system of machine tools as a functional part of linear motion [1]. With the continuous improvement of manufacturing requirements for high-end CNC machine tool performance, high-speed cutting requires machine tools to improve production efficiency and reduce production costs under the premise of ensuring the quality of part processing. It is moving toward high-speed and precise directions. However, the tracking accuracy of the feed system is also affected by factors such as the mechanical dynamic characteristics of roller screws, the control algorithm used, external disturbances, and the feedback quality of sensors. During the high-speed cutting process, especially under heavy load and high acceleration conditions, the vibration mode of the feed system is stimulated, and system deformation and vibration will be particularly serious, resulting in an unstable control system and limiting the servo bandwidth [2]. In addition, a ball screw feed system is a time-varying system with uncertainty, and its vibration mode changes with the position of the table and the quality of the loaded workpiece [1,3]. During the cutting process, the feed system is also affected by external disturbances such as cutting force and nonlinear friction [4]. At the same time, there are random interferences and noises in the feedback signals collected by the controller from the rotary encoder and the grating ruler. Therefore, to improve the tracking accuracy of a ball screw feed system, it is necessary to fully study its dynamic characteristics and establish an accurate control model. Secondly,

the servo control algorithm is designed according to the control model to achieve two main goals: (1) it can track the ideal reference trajectory quickly and accurately in a high-speed environment, reduce the tracking error, and improve the bandwidth of the servo system, and (2) it can suppress the vibration of the system structure, and has robustness to the time-varying uncertainty of the system, external disturbances, and unmodeled dynamics.

Classical control methods, such as PID or P-PI (proportional integral) cascade control, have the advantages of simple principle, convenient use, and strong robustness, among others, and these methods have been widely used in industrial motion control [5,6]. However, a traditional control algorithm only considers the control model of the rigid-body dynamics of the system, ignoring the significant influence of structural vibration on the servo bandwidth [1,7]. In addition, a traditional controller is still limited by the uncertainty and nonlinear factors of the system. To obtain a higher servo system bandwidth and better tracking accuracy of the feed system, researchers have conducted extensive research work in this field in recent years, and a large number of advanced control algorithms have emerged [8–11]. Erkorkmaz and Kamalzadeh [7] first designed an adaptive sliding mode control to control the rigid body motion of ball screw drives, and the notch filtering and active cancellation techniques were used to compensate for the first-order vibration mode in the control law. In order to accurately describe the axial vibration mode of the ball screw feed system, a two-degree-of-freedom model was applied to the motion controller design to achieve high positioning bandwidth [12]; furthermore, Erkorkmaz and Kamalzadeh modeled the lead errors of the ball screw and removed them from the loop by offsetting their effect from the command trajectory and position feedback signals. After that, various control methods were used in the controller design for the two-degree-of-freedom model of the ball screw feed system, such as discrete-time sliding mode control [13], backstepping sliding mode control [14], pole placement technique [15] and optimal non-collocated control [16,17] et al. Altintas and Khoshdarregir [18] presented a vibration avoidance and contouring error compensation algorithm for feed drives; they reduced residual vibrations in CNC machine tools by applying input shaping filters on the reference commands. Friction compensation is also one of the main research directions for motion control of ball screw feed systems. To compensate for the contour tracking errors caused by friction forces only, Jamaludin et al. [19] proposed a method that combines feedforward based on the Generalized Maxwell-slip friction model and the disturbance observer. Fujimoto [20] introduced a repetitive perfect tracking controller with n-times learning filter to compensate for ball screw friction without a specific friction model. For precise control of ball-screw-driven stages, Hayashi et al. [21,22] used projection-based iterative learning control to deal with both variations in position reference and rolling friction compensation. In addition, more advanced methods were used for tracking and vibration control of ball screw feed systems. Tsai et al. [23] proposed an integrated iterative learning control with empirical mode decomposition to filter out undesired signals from the reference commands, thereby avoiding the resonance modes excitation in high-precision machining. To compensate for unmodeled dynamics, parameter perturbations, variable cutting load, and other uncertainties of ball screw drives, an active-disturbance-rejection control (ADRC) and a proportional-integral (PI) control are employed by Zhang [24] to ensure the performance of the closed-loop system. Rajabi et al. [25] proposed a trajectory tracking control of a ball-screw-driven servomechanism based on the sliding mode approach with state estimation using an extended Kalman filter/unscented Kalman filter. A constrained nonsingular terminal sliding mode controller with a super-twisting state observer was proposed by Park et al. [26] to compensate for unknown dynamics and unmeasured velocity signals in the ball screw drive system. To increase the bandwidth of the position loop without any extra sensor or actuator, Sun et al. [27] added a weakly set motor speed controller and a disturbance observer with the feedback velocity of the machine table into the traditional PD controller. Simba et al. [28] proposed an iterative learning contouring controller consisting of a classical PD controller and disturbance observer, and the proposed controller was evaluated experimentally by using a typical sharp-corner trajectory. Li et al. [29] presented a dynamic model of ball screw

drives as a feedforward compensation to offset the position commands and thus reduce dynamic mechanical tracking errors. Yang et al. [30] proposed a dual-position feedback control method by introducing position information on the drive side with a filter in the position loop feedback channel and designed an adaptive backlash error compensation method that could reduce over-quadrant errors. Then, Shirvani et al. [31] used adaptive feedforward cancellation to address the problem of harmonic positioning error suppression in ball screw drives. Recently, Huang et al. [32] used an adaptive sliding mode control based on fuzzy exponential convergence law to solve the sliding mode jitter problem and to improve the tracking performance of the ball screw feed system.

The controller designs mentioned above did not explicitly focus on the dynamic time-variant characteristics of ball screw drives. The gain-scheduled methods based on a linear parameter-varying (LPV) system [33–36] can cope with time-varying characteristics, but their applications for industrial ball screw drives are complicated. In this paper, the time-varying characteristics of a ball screw feed system are fully considered as part of the total perturbations of the system. Because of the variation in parameters of the system, external disturbances and other disturbances exist in both the motor and table sides at the same time; therefore, the ball screw feed system also has system perturbations that satisfy or dissatisfy the matching conditions. To compensate for system perturbations, a generalized extended state observer is used to observe both system perturbations and each state variable. Finally, an improved integral sliding mode controller is designed based on the observed values, which can compensate for the system's matched and mismatched perturbations at the same time. Vibration compensation is designed to address first-order axial vibration of the system, and a controller is proposed that can track the ideal reference trajectory quickly and accurately, suppresses the vibration of the system structure, and is robust to the time-varying uncertainty of the system, external disturbances, and unmodeled dynamics. Finally, simulation and experimental comparisons between the proposed controller and an ordinary ISMC are presented.

The structure of this paper is organized as follows: The model for the flexible ball screw drive system is presented in Section 2. In Section 3, a tracking controller based on ISMC is designed; then, a GESOISMC is designed for both tracking performance and disturbance suppression; finally, a vibration compensation is designed for structural vibration suppression. The experimental setup, simulation, and results are presented in Section 4. The conclusions are drawn in Section 5.

2. Ball Screw Drive Model

Figure 1 shows the structure of a typical ball screw feed system. Such a system is usually composed of servo motors, lead screws, nuts, linear guides, worktables, bearings, and couplings. During the operation of the system, the control voltage output by the controller acts on the servo motors, and the servo motors generate a torque to drive the screws to rotate. Then, the rotating motion is converted into the linear motion of the tables by the nuts. Afterward, the rotational displacement and speed of the motors and the linear displacement and speed of the tables are, respectively, transmitted as feedback to the system by the rotary encoder and the linear grating ruler. In addition, during operation, the system is also affected by external disturbances, including cutting forces along the screw axis and nonlinear friction. In the process of high-speed operation, the axial vibration mode of the system is excited, which will deteriorate the stability of the closed-loop system and greatly limit the dynamic accuracy of the ball screw drives.

To accurately describe the rigid body and first-order vibration mode characteristics of the system, the system can be simplified into a two-degree-of-freedom mass model, as shown in Figure 2, which not only can effectively describe the system's characteristics but can also be easily applied to the controller design. According to the two-degree-of-freedom mass model, the kinetic equation of the system can be expressed as follows [37]:

$$\begin{aligned}
m_2\ddot{x}_2 &= -b_2\dot{x}_2 + k(x_1 - x_2) + c(\dot{x}_1 - \dot{x}_2) + d_2(t) \\
m_1\ddot{x}_1 &= -b_1\dot{x}_1 + k(x_2 - x_1) + c(\dot{x}_2 - \dot{x}_1) + u + d_1(t)
\end{aligned} \tag{1}$$

where m_1 represents the equivalent mass of the rolling element of the system; m_2 is the equivalent mass of the moving components of the system; b_1 is the viscous damping of motors and bearings, while b_2 is the viscous damping of linear guides; k is the overall axial stiffness of the system, including the axial stiffness of screw nuts, couplings, and angular contact bearings; c is the damping of the preload nut; u is the motor torque control instruction; d_1 and d_2 represent external equivalent disturbances acting on the rotating and moving components, respectively; x_1 and x_2 indicate the rotation displacement of the ball screw and the linear displacement of the table, respectively; and $\dot{x}_1$ and $\dot{x}_2$ are, respectively, the rotation speed of the ball screw and the linear speed of the table. According to Equation (1), the state-space expression of the system can be expressed as

$$\begin{cases} \dot{x} = Ax + Bu + Dd \\ y = Cx \end{cases} \tag{2}$$

and expanded as

$$\begin{bmatrix} \dot{x}_2 \\ \dot{x}_1 \\ \ddot{x}_2 \\ \ddot{x}_1 \end{bmatrix} = \begin{bmatrix} 0 & 0 & 1 & 0 \\ 0 & 0 & 0 & 1 \\ -\dfrac{k}{m_2} & \dfrac{k}{m_2} & -\dfrac{b_2+c}{m_2} & \dfrac{c}{m_2} \\ \dfrac{k}{m_1} & -\dfrac{k}{m_1} & \dfrac{c}{m_1} & -\dfrac{b_1+c}{m_1} \end{bmatrix} \begin{bmatrix} x_2 \\ x_1 \\ \dot{x}_2 \\ \dot{x}_1 \end{bmatrix} + \begin{bmatrix} 0 \\ 0 \\ 0 \\ \dfrac{1}{m_1} \end{bmatrix} u + \begin{bmatrix} 0 & 0 \\ 0 & 0 \\ \dfrac{1}{m_2} & 0 \\ 0 & \dfrac{1}{m_1} \end{bmatrix} \begin{bmatrix} d_2(t) \\ d_1(t) \end{bmatrix}$$

$$\begin{bmatrix} y_1 \\ y_2 \end{bmatrix} = \begin{bmatrix} 0 & 1 & 0 & 0 \\ 1 & 0 & 0 & 0 \end{bmatrix} \begin{bmatrix} x_2 \\ x_1 \\ \dot{x}_2 \\ \dot{x}_1 \end{bmatrix} \tag{3}$$
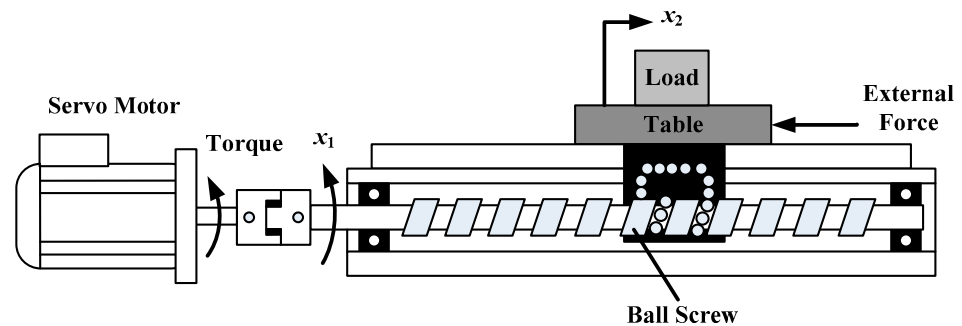

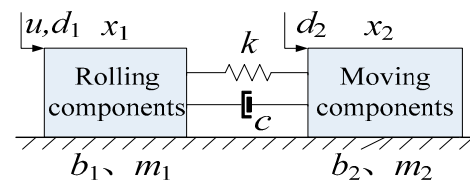**Figure 1.** Schematic representation of a ball screw drive system.

Figure 2. Two-degree-of-freedom mass model.

By imposing the Laplace transform on Equation (3) and combining similar terms, the dynamic transfer function between the control signal input, external disturbances, motor output, and table can be obtained as follows:

$$\begin{bmatrix} y_1 \\ y_2 \end{bmatrix} = \begin{bmatrix} G_{11}(s) & G_{12}(s) & G_{13}(s) \\ G_{21}(s) & G_{22}(s) & G_{23}(s) \end{bmatrix} \begin{bmatrix} u \\ d_1 \\ d_2 \end{bmatrix}$$

$$= \frac{1}{Q(s)} \begin{bmatrix} m_2 s^2 + (b_2 + c)s + k & m_2 s^2 + (b_2 + c)s + k & k + cs \\ k + cs & k + cs & m_1 s^2 + (b_1 + c)s + k \end{bmatrix} \begin{bmatrix} u \\ d_1 \\ d_2 \end{bmatrix} \qquad (4)$$

and $Q(s)$ is

$$\begin{aligned} Q(s) = \ & m_1 m_2 s^4 + (m_2 b_1 + m_2 c + m_1 b_2 + m_1 c)s^3 \\ & + (b_1 b_2 + b_1 c + b_2 c + m_2 k + m_1 k)s^2 + (b_1 k + b_2 k)s \end{aligned} \qquad (5)$$

where $G_{11}(s)$ and $G_{21}(s)$, respectively, represent the transfer functions between the motor drive torque, the rotation displacement, and the linear displacement of the table. $G_{11}(s)$ and $G_{21}(s)$ are, respectively, the transfer functions between external disturbances d_1 and the rotation displacement and linear displacement of the table. Similarly, $G_{13}(s)$ and $G_{23}(s)$ are the transfer functions between external disturbances d_2 and the rotation displacement and linear displacement of the table, respectively. Therefore, Equation (5) describes the flexible and dynamic characteristics of the ball screw feed system in the form of a transfer function.

In actual operation, stiffness k and damping c vary due to variations in the table position and the workpiece mass, and the equivalent mass m_1 and m_2 also change due to variations in the workpiece mass. Therefore, when the table position and the workpiece mass fluctuate within a certain range, the four physical parameters m_1, m_2, k, and c exhibit uncertainties. If the above physical parameter values vary over a bounded range, there are uncertainties of 40%, 40%, 30%, and 20% for m_1, m_2, k, and c, respectively, the frequency response curve of the transfer function $G_{21}(s)$ exhibits the characteristics shown in Figure 3. Due to the uncertainties of the parameters, the frequency of the amplitude peak fluctuates within a certain range, which indicates that the first-order natural frequency of the system changes with variations in the equivalent mass, stiffness, and damping of the system.
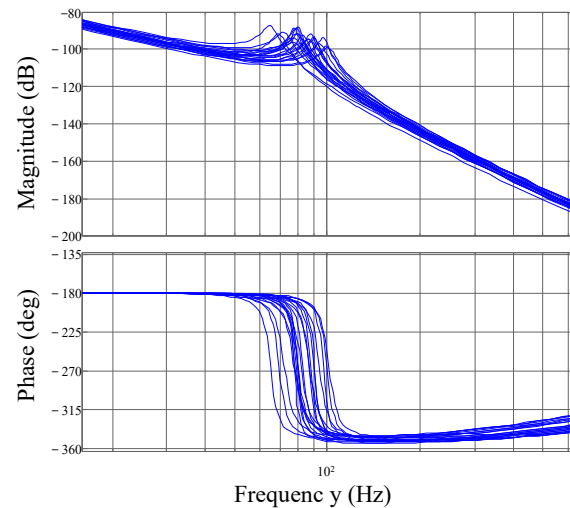

Figure 3. Frequency response curve of transfer function $G_{21}(s)$ with parameter uncertainty.

The parameter uncertainties of the ball screw feed system are added to the spatial expression (2) as a part of system perturbations, and the system can be expressed as follows:

$$\begin{cases} \dot{x} = Ax + Bu + Df(x, d(t), t) \\ y = Cx \\ y_2 = c_2 x \end{cases} \qquad (6)$$

where, $f(x, d(t), t) = [f_2\, f_1]^{\mathrm{T}}$ represents the total perturbations to the feed system, including external disturbances, parameter uncertainties, and unmodeled dynamics. External disturbances usually include the nonlinear friction existing in the system and the cutting force in the mechanical cutting process. Parameter uncertainties are mainly caused by variations in the machined workpiece mass and table position. Unmodeled dynamics mainly include high-frequency dynamics, lead error of the lead screw, and axial elastic deformation. So f_1 represents the total perturbations existing in the rotational motion of the feed system, which exists in the same channel as the motor input signal u, and thus, the matching conditions are satisfied. On the contrary, f_2 represents the total perturbations existing in the linear motion of the feed system, which is not in the same channel as the motor input signal u, and thus, it does not meet the matching conditions. Both f_1 and f_2 are bounded.

3. Integral Sliding Mode Control with Generalized Extended State Observer

3.1. Design of Integral Sliding Mode Controller for Flexible Drives

When the ordinary sliding mode control tracks any trajectory, it will appear to have a steady-state error if there are some external disturbances and cannot achieve the desired tracking performance. The integral sliding mode control can enhance the initial state of the system located on the sliding mode surface, effectively eliminating the steady-state error of the system [38]. Moreover, the integral sliding mode control is applicable to both minimum-phase systems and non-minimum-phase systems and is robust to matched perturbations of such systems [39]. Therefore, for the feed system described in formula (6), an integral sliding mode controller is designed without considering mismatched perturbations. Then, the system can be expressed as follows:

$$\begin{cases} \dot{x} = Ax + B(u + f_1(x, d(t), t)) \\ y = Cx \end{cases} \tag{7}$$

To eliminate the influence of f_1 on system performance, the integral sliding mode surface can be designed as follows:

$$\sigma(x, t) = C_I(x(t) - x_0) - C_I \int_0^t (A + BK_I)x(\tau)d\tau$$
$$x_0 = x(0) \tag{8}$$

where $C_I \in \mathbb{R}^{1 \times 4}$ is an integer vector and an appropriate C_I is designed to ensure that $C_I B$ is a positive definite non-singular matrix [40]; x_0 is the initial state of the system state variable; and $K_I \in \mathbb{R}^{1 \times 4}$ is the coefficient matrix that needs to be designed. When the system state is in the corresponding sliding mode plane, its condition is $\sigma(x,t) = \dot{\sigma}(x,t) = 0$, and then

$$\dot{x}(t) = (A + BK_I)x(t) \tag{9}$$

To obtain the desired control effect, appropriate K_I is designed so that $A + BK_I$ is the Hurwitz matrix. It should be noted that the linear term $C_I(x(t) - x_0)$ is continuous in the integral sliding mode surface, and the integral term $C_I \int_0^t (A + BK_I)x(\tau)d\tau$ is also continuous. When each state of the system Equation (7) is switched, the integral sliding mode surface remains continuous [41]. The state variable error e and the state variable reference value x_{ref} are defined as follows:

$$e(t) = x(t) - x_{ref}(t) \tag{10}$$

Similarly, the controller is designed to minimize the error e of the state variable; thus, the integral sliding mode surface can be redesigned as

$$\sigma(e, t) = C_I(e(t) - e_0) - C_I \int_0^t (A + BK_I)e(\tau)d\tau$$
$$e_0 = e(0) \tag{11}$$

The derivative of the integral sliding mode surface (11) is obtained as

$$\dot{\sigma} = C_I \dot{e} - C_I(A + BK_I)e = C_I(\dot{x} - \dot{x}_{ref}) - C_I(A + BK_I)e \tag{12}$$

Substituting system (7) into Equation (12) yields

$$\dot{\sigma} = C_I[(Ax + Bu + Bf_1) - \dot{x}_{ref} - Ae - BK_Ie] = C_I[Ax_{ref} + Bu + Bf_1 - \dot{x}_{ref} - BK_Ie] \tag{13}$$

To satisfy the sliding mode condition, the control law u can be designed as

$$u = -(C_IB)^{-1}(C_IAx_{ref} - C_I\dot{x}_{ref}) + K_Ie - (\eta + \overline{f}_1)\text{sgn}(\sigma) \tag{14}$$

where $\overline{f}_1$ is the upper bound of the perturbation f_1 and can be expressed as $\overline{f}_1 \geq |f_1|$; sgn() represents the sign function; and $\eta > 0$ is the parameter to be designed.

The control law u (14) is substituted into Equation (13) as follows:

$$\dot{\sigma} = C_IB[f_1 - (\eta + \overline{f}_1)\text{sgn}(\sigma)] \tag{15}$$

The Lyapunov function is defined as

$$V_1 = \frac{1}{2}\sigma^2 \tag{16}$$

The derivative of the Lyapunov function (16) is taken as

$$\dot{V}_1 = \sigma\dot{\sigma} = C_IB(\sigma f_1 - \overline{f}_1|\sigma| - \eta|\sigma|) \leq 0 \tag{17}$$

Therefore, according to the Lyapunov stability theory, the designed integral sliding mode controller meets the condition of reaching equilibrium and is asymptotically stable.

3.2. Design of Generalized Extended State Observer for Flexible Drives

The standard extended state observer method is only available for the integral chain system [42], but the ball screw feed system (6) does not satisfy the standard form. On the other hand, ESO cannot observe disturbances that do not satisfy the matching conditions. To observe both matched and mismatched perturbations contained in the flexible model of the ball screw feed system, it is necessary to design a generalized extended state observer based on the system in Equation (6). First, the total perturbation f of the system is taken as the extended state variable of the system as follows:

$$x_5 = f_2, x_6 = f_1 \tag{18}$$

Combined with the new state variables x_5 and x_6 and system Equation (6), the new extended system can be expressed as

$$\begin{cases} \dot{\overline{x}} = \overline{A}\overline{x} + \overline{B}u + Eh(t) \\ y = \overline{C}x \end{cases} \tag{19}$$

where

$$\overline{x} = \begin{bmatrix} x \\ x_5 \\ x_6 \end{bmatrix}, h(t) = \frac{df}{dt} \tag{20}$$

The system matrix can be expressed as

$$\overline{A} = \begin{bmatrix} A_{4\times4} & D_{4\times2} \\ 0_{2\times4} & 0_{2\times2} \end{bmatrix}_{6\times6}, \overline{B} = \begin{bmatrix} B_{4\times1} \\ 0_{2\times1} \end{bmatrix}_{6\times1}, E = \begin{bmatrix} 0_{4\times2} \\ I_{2\times2} \end{bmatrix}_{6\times2}, \overline{C} = \begin{bmatrix} C_{2\times4} \\ 0_{2\times2} \end{bmatrix}^T_{2\times6} \tag{21}$$

For system Equation (19), the generalized extended state observer can be designed as follows:

$$\begin{cases} \dot{\hat{\overline{x}}} = \overline{A}\hat{\overline{x}} + \overline{B}u + L(y - \hat{y}) \\ \hat{y} = \overline{C}\hat{\overline{x}} \end{cases} \tag{22}$$

where $\hat{\overline{x}} = [\hat{x}^T \ \hat{x}_{n+1} \ \hat{x}_{n+2}]^T$, and $\hat{\overline{x}}$, $\hat{x}$, $\hat{x}_5$, and $\hat{x}_6$ represent estimates of the state variables $\overline{x}$, x, x_5, and x_6 of the extended system Equation (19), respectively. Matrix L is the observer gain of dimension 6×2, and selecting an appropriate observer gain can ensure the convergence of the system. It is supposed that the perturbation function f satisfies the following conditions:

(1) Both f_1 and f_2 are bounded;

(2) In the steady state, f_1 and f_2 are constant, that is, $\lim_{t\to\infty} f = \lim_{t\to\infty} h_{(t)} = 0$, and $\lim_{t\to\infty} f = D_c$, where D_c is a constant matrix.

The estimated error of each state variable of the observer is defined as

$$\begin{cases} e_x = \hat{x} - x \\ e_{f2} = \hat{f}_2 - f_2 = \hat{x}_5 - x_5 \\ e_{f1} = \hat{f}_1 - f_1 = \hat{x}_6 - x_6 \end{cases} \tag{23}$$

Combined with Equations (19), (22) and (23), the estimated error equation can be expressed as

$$\dot{e}_{GESO} = A_e e_{GESO} - Eh(t) \tag{24}$$

In this equation,

$$e_{GESO} = \begin{bmatrix} e_x \\ e_{f2} \\ e_{f1} \end{bmatrix}, A_e = \overline{A} - L\overline{C} \tag{25}$$

If an appropriate observer gain matrix L is selected and the matrix A_e is guaranteed to be a Hurwitz matrix, then the observation error e_{GESO} of the extended state observer is also bounded for any bounded $h(t)$ [43].

3.3. Integral Sliding Mode Controller with GESO for Flexible Drives

An integral sliding mode controller is designed for the flexible model of the ball screw feed system based on Equation (6), which can simultaneously compensate for two kinds of system perturbations. Combined with the GESO design, the new integral sliding mode surface designed for the state variable error e can be expressed as follows:

$$\overline{\sigma}(e, t) = C_I(e(t) - e_0) - C_I \int_0^t (A + BK_I)e(\tau)d\tau + C_d\hat{f} \\ e_0 = e(0) \tag{26}$$

where $C_d \in \mathbb{R}^{1\times2}$ is the positive integer vector to be designed, and $\hat{f} = [\hat{f}_2 \ \ \hat{f}_1]^T$ is the observed value of system disturbance obtained via GESO observation.

The derivative of the integral sliding mode surface (26) is obtained as

$$\dot{\overline{\sigma}} = C_I\dot{e} - C_I(A + BK_I)e + C_d\dot{\hat{f}} = C_I(\dot{x} - \dot{x}_{ref}) - C_I(A + BK_I)e + C_dL_f(y - \hat{y}) \tag{27}$$

By bringing Equation (6) into Equation (27),

$$\dot{\overline{\sigma}} = C_I[Ax_{ref} + Bu + Df - \dot{x}_{ref} - B_uK_Ie] - C_dL_fCe_x \tag{28}$$

In the above formula, L_f is the 5th and 6th row of the designed observer gain L.

To satisfy the sliding mode condition and compensate for the perturbations f, which satisfy and dissatisfy the matching conditions, the control law $u_{GEOISMC}$ can be designed as follows:

$$u_{GESOISMC} = -(C_IB)^{-1}(C_IAx_{ref} - C_I\dot{x}_{ref}) + K_Ie + K_d\hat{f} - \eta\mathrm{sgn}(\overline{\sigma}) \tag{29}$$

where K_d is the disturbance compensation gain to be designed. The control law $u_{GEOISMC}$ (29) is substituted into Equation (28) as

$$\dot{\overline{\sigma}} = C_I[(BK_d + D)f + BK_d e_f - B\eta\text{sgn}(\overline{\sigma})] - C_d L_f C e_x \tag{30}$$

where K_d designed in this section can be expressed as

$$K_d = -(C_I B)^{-1} C_I D \tag{31}$$

It will be shown next that the matched and mismatched perturbations can be eliminated from the output channel in a steady state by the proposed control law.

3.4. Stability and Perturbation Rejection Analysis

The disturbance compensation gain K_d obtained from Equation (31) is substituted into Equation (30) as follows:

$$\dot{\overline{\sigma}} = C_I D e_f - C_f L_f C e_x - C_I B\eta\text{sgn}(\overline{\sigma}) \tag{32}$$

It can be seen from Equation (32) that the total perturbations of the system are eliminated from the sliding mode surface.

Proof. The Lyapunov function is defined as

$$\overline{V}_1 = \frac{1}{2}\overline{\sigma}^2 \tag{33}$$

The derivative of the Lyapunov function (33) is taken as

$$\dot{\overline{V}}_1 = \overline{\sigma}\dot{\overline{\sigma}} = C_I B_u(\overline{\sigma}(-K_d e_f - (C_I B_u)^{-1} C_d L_f C e_x) - \eta|\overline{\sigma}|) \tag{34}$$

According to Equation (34), the value of $(-K_d e_f - (C_I B_u)^{-1} C_d L_f C e_x)$ depends on the observation error e_{GESO} of the generalized extended state observer for each state variable. According to Section 3.1, for ball screw drives with bounded perturbations f, since the designed GESO observation error e_{GESO} converges to an arbitrarily small predictable range in a finite time, there must be a constant $\delta > 0$ that satisfies $\delta = \sup_{t>0}|-K_d e_f - (C_I B_u)^{-1} C_d L_f C e_x|$.

Therefore, if $\eta > \delta$ is guaranteed to result in $\dot{\overline{V}}_1 \leq 0$, then the designed integrated sliding mode controller can satisfy the reaching condition and ensure asymptotic stability of the system with both matched and mismatched perturbations.

To eliminate the perturbations presented in the system output under steady-state conditions, C_I can be designed as

$$C_I = c_2(A + BK_I)^{-1} \tag{35}$$

In the case of convergence of the designed GESO, if the matrices A_e and $A_I = A + BK_I$ are Hurwitz matrices, and $c_o A_I^{-1}B$ is invertible, by designing integrated sliding mode control laws (29), (31), and (35) based on GESO, the perturbations existing in the output channel of the ball screw drive system (6) can be eliminated under steady-state conditions.

Proof. By bringing the control law (29) into the ball screw feed system (6), the system state variables can be expressed as

$$x = (A + BK_I)^{-1}[\dot{x} - B(-(C_I B)^{-1}(C_I A x_{ref} - C_I \dot{x}_{ref}) - K_I x_{ref}) - BK_d e_f - (D + BK_d)f + B\eta\text{sgn}(\overline{\sigma})] \tag{36}$$

By bringing system Equation (6), Formula (31), and Formula (35) into Formula (36),

$$y_2 = c_2(A + BK_I)^{-1}[\dot{x} - \dot{x}_{ref} + D e_f + B\eta\text{sgn}(\overline{\sigma})] + c_2 x_{ref} \tag{37}$$

According to Equation (37), the total perturbations of the flexible ball screw feed system are eliminated from the output channel. The appropriate selection of observer gain

matrix L and feedback control gain K_I guarantees that A_e and $A_I = A + BK_I$ are Hurwitz matrices, and $c_2 A_I^{-1}B$ is reversibly available according to the following equation:

$$\lim_{t\to\infty} \dot{x}(t) = \dot{x}_{ref}, \lim_{t\to\infty} e_{GESO}(t) = 0, \lim_{t\to\infty} \sigma(t) = 0 \tag{38}$$

Then, the combination of formula (37) and (38) results in

$$\lim_{t\to\infty} y_2(t) = y_{2ref} \tag{39}$$

where y_{2ref} is the reference value of the table position. Formula (39) shows that the designed GESO-based integral sliding mode controller can eliminate perturbations in the table position output channel of the flexible ball screw feed system (6) under steady-state conditions, and the feed system output accurately tracks its reference value.

When each state variable x of the system is unknown, the system state variable $\hat{x}$ obtained via GESO can be used as controller feedback. In this case, the integral sliding mode surface can be expressed as

$$\hat{\sigma}(e,t) = C_I(\hat{e}(t) - e_0) - C_I \int_0^t (A + BK_I)\hat{e}(\tau)d\tau + C_d \hat{f}$$
$$e_0 = e(0) \tag{40}$$

In the formula, $\hat{e} = \hat{x} - x_{ref}$. Then, the integral sliding mode control law $u_{GEOISMC}$ based on GESO can be expressed as

$$u_{GESOISMC} = -(C_I B)^{-1}(C_I A x_{ref} - C_I \dot{x}_{ref}) + K_I \hat{e} + K_d \hat{f} - \eta \text{sgn}(\hat{\sigma}) \tag{41}$$

3.5. Vibration Compensation Design

When the frequency of external disturbances of the system is close to the first-order axial vibration mode of the ball screw feed system, especially when the friction force and cutting force are transient, the axial vibration of the system is excited. When the feed system vibrates in the first-order axial vibration mode, the axial vibration feedback of the rotary encoder is much smaller than that of the linear grating. According to this phenomenon, vibration compensation is added to the controller.

The axial deformation of the system is characterized by the difference between the grating rule feedback displacement $y_2[m]$ and the rotary encoder feedback displacement $y_2[m]$. To separate the exact axial vibration signal from the steady-state axial deformation, the detected displacement difference signal is passed through a high-pass filter whose cutoff frequency ω_c is slightly less than the first-order axial vibration mode ω_n of the feed system. In order to offset the axial vibration occurring at the free end of the ball screw, the vibration compensation signal is designed to multiply the displacement difference signal through high-pass filtering by a proportional gain K_p, which can be expressed as

$$u_{VC} = K_p \frac{s^2}{(s + \omega_c)^2}(y_2 - y_1) \tag{42}$$

Finally, the integral sliding mode controller u with an extended state observer and vibration compensation designed for the flexible model of the ball screw feed system can be expressed as

$$u = u_{GEOISMC} + u_{VC} \tag{43}$$

This approach was found to be effective in damping out the first-order vibration mode. The high-pass filter gain drops below -3 dB after ω_n, making it difficult to dampen out the second and higher order modes.

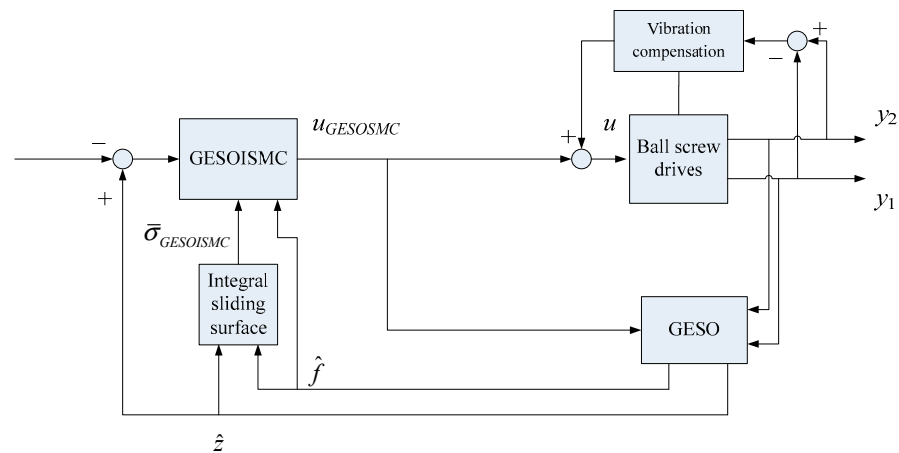The overall structure diagram of the closed-loop system is shown in Figure 4.

Figure 4. Structural block diagram of GESO-based ISMC with vibration suppression.

4. Simulation and Experimental Verification

4.1. Experimental Setup and Modeling

The structure of the high-speed ball screw feed experimental system is shown in Figure 5. To reduce vibration, the bed of the feed bench is made of granite. The system is powered by a 9 kW servo motor, and the maximum output torque is 85.8 [Nm], the rated output torque is 28.6 [Nm], the matching servo drive is set to torque control mode, and the analog control voltage is ±8 [V]. For safety reasons, the torque output is limited to 20% of the maximum output torque during parameter identification so that the motor current constant and torque constant are 2.145 [Nm/V]. The lead and diameter of the ball screw pair are 20 [mm] and 20 [mm], respectively, and the total length of the screw is 1044 [mm], of which the thread length is 867 [mm]. The total mass of the table is 50 [kg]. An incremental linear grating ruler is installed on one side of the table to feedback the linear displacement of the table. The ball screw is equipped with an incremental rotary encoder near the motor side, which is used to feedback the rotary displacement of the screw. The feedback signal is subdivided through the IBV subdivision box. The subdivision box selects a subdivision 400 times. After subdivision, the signal resolution of the rotary encoder is 2.5 [nm], and the signal separation rate of the linear grating ruler is 12.5 [nm]. The system controller adopts the dSPACE DS1103 real-time simulation system.
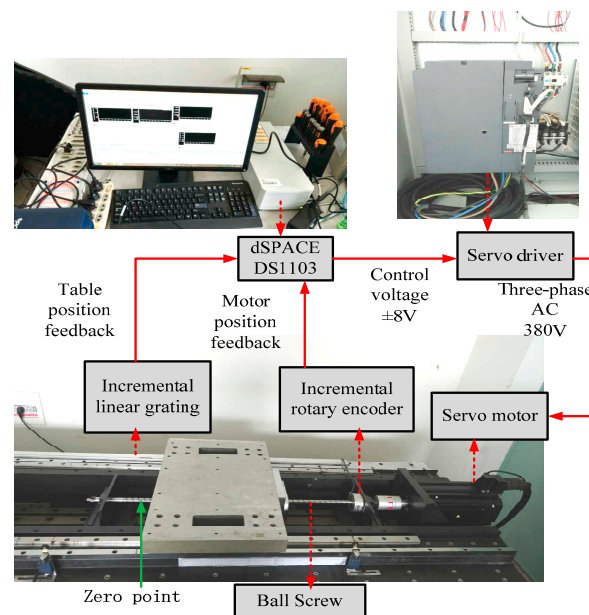

Figure 5. High-speed ball screw feed experimental system.

The parameters of the flexible model of the ball screw feed system were identified through a sinusoidal sweep frequency test on the above test equipment. The open-loop frequency response function (FRF) of the system obtained via the sweep frequency experiment is shown in Figure 6. The parameters in the system state-space Equation (3) were obtained through fitting using the least-squares method, and the results are shown in Table 1.
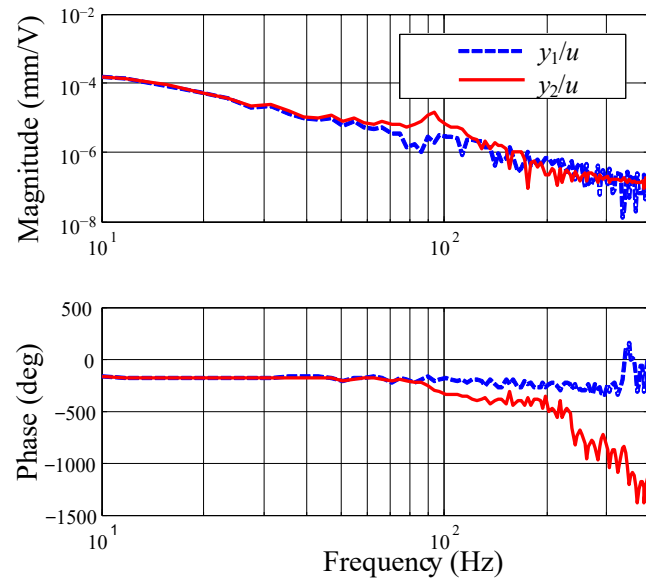

Figure 6. Response of the test system in the open-loop frequency domain.

Table 1. Parameters of flexible body model of the ball screw feed system.

m_1 (V·s²/m)	m_2 (V·s²/m)	b_1 (V·s/m)	b_2 (V·s/m)	k (V/m)	c (V·s/m)
0.6512	0.0771	4.1571×10^{-4}	0.8052	2.1153×10^{4}	2.6775

As shown in Figure 6, the structural resonance is located at $\omega_n = 94.7$(Hz), which is the first-order axial vibration mode of the experimental system and is usually attributed to the flexibility of the bearing and lead screw. This vibration mode is easily excited by the motor torque and dominates the factors that affect the tracking accuracy of the table. The sensitivity of the ball screw feed system to changes in the workpiece mass is very important. During machining, the load (table) inertia changes with the cutting process of the material. Therefore, this work considered changes in the dynamic characteristics of the ball screw feed experimental system under three different masses. Different masses with loads of 0 kg, 25 kg, and 50 kg were placed on the worktable. The open-loop frequency-domain response curves obtained through plotting the experimental data and parameter fitting are shown in Figure 7. As observed, the first-order vibration mode of the system changes with a change in load mass, the natural frequency decreases gradually with an increase in mass, and the system stiffness also decreases gradually. Therefore, the designed controller must be robust to the parameter uncertainties caused by this situation.
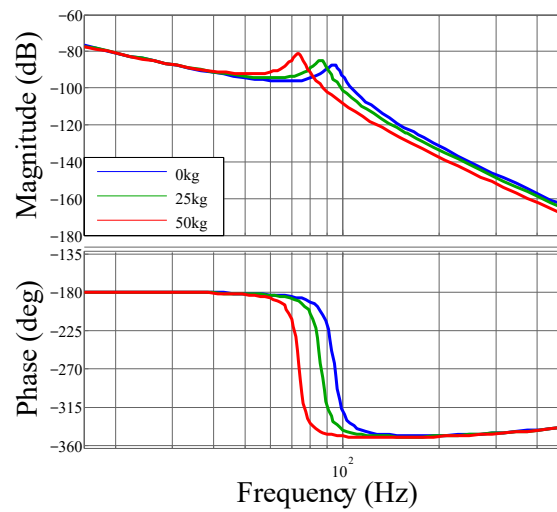
Figure 7. System frequency response curves under different load masses.

4.2. Simulation Verification

The reference trajectory adopted in the simulation has a maximum stroke of 80 [mm], a maximum speed of 250 [mm/s], and a maximum acceleration of 0.25 g [mm/s^2]. The reference trajectory diagram obtained from the simulation is shown in Figure 8. The simulation was carried out in the Matlab/Simulink environment, and the solution algorithm was selected as ode1 with a frequency of 20 [kHz]. The flexible control model of the ball screw feed system described in Figure 5 of the controlled object uses the parameters of the two-degree-of-freedom quality model presented in Table 1. The comparison objects are as follows:

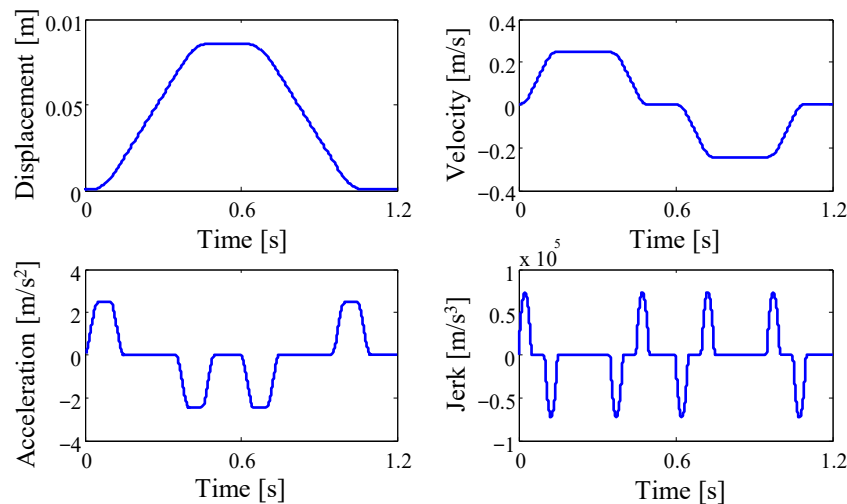(1) Case 1: GESOISMC with vibration compensation;
(2) Case 2: ISMC.

Figure 8. Reference trajectory.

4.2.1. Tracking Performance Only with Matched Perturbation

To verify the robustness of the designed controller against matched perturbation, a sinusoidal signal $f_1 = 1.5\sin(2\pi t)$ was added to the simulation as an external disturbance. The tracking error and control signal obtained from the simulation are shown in Figure 8.

As shown in Figure 9, both controllers can fully compensate for the matched external disturbance in the system, maintain the tracking accuracy of the system, and keep the tracking error consistent with the scenario when there is an absence of disturbance, with

the maximum tracking error still being 1.575 [μm]. The simulation results show that the two controllers have strong robustness to the matched external disturbance.
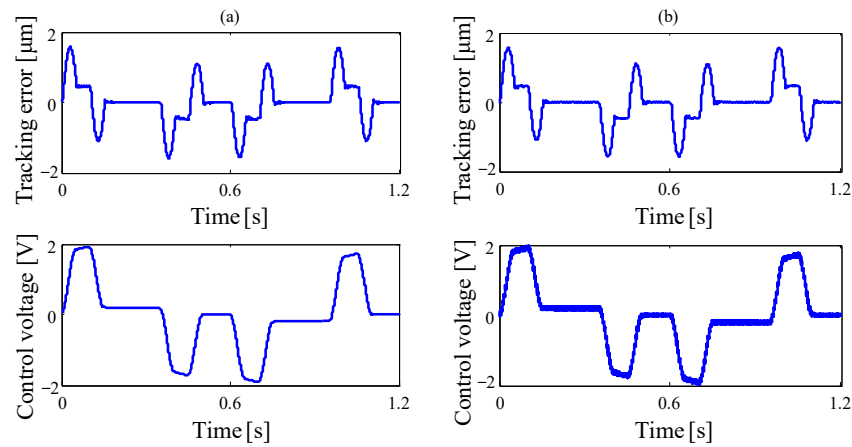

Figure 9. Simulation results of tracking performance only with matched perturbation: (**a**) Case 1 and (**b**) Case 2.

4.2.2. Tracking Performance with Matched and Mismatched Perturbations

To verify the robustness of the designed controller against both matched and mismatched perturbations, a mismatched sinusoidal signal $f_2 = 1.2\sin(\pi t)$ and a matched sinusoidal signal $f_1 = 1.5\sin(2\pi t)$ were added in the simulation process at the same time. The tracking error and control signal obtained from the simulation are shown in Figure 10.
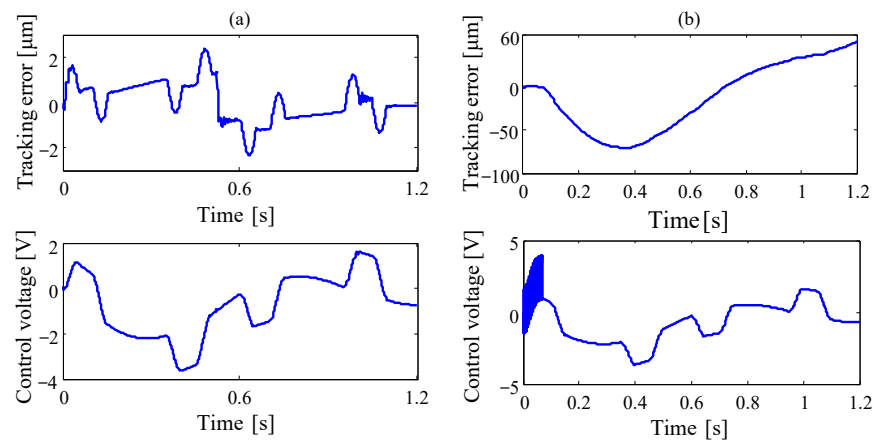

Figure 10. Simulation results of tracking performance with matched and mismatched perturbations: (**a**) Case 1 and (**b**) Case 2.

As shown in Figure 10b, in the case of an interference that does not meet the matching conditions, if the ISMC cannot eliminate the influence of disturbances existing in the system output completely, the tracking error greatly increases, and the maximum tracking error is 71.076 [μm]. Moreover, the tracking error curve is completely deformed due to the existence of mismatched external disturbances, and the position of the table does not return to the original point after the movement, with a positioning error of 71.076 [μm]. In contrast, the GESOISMC can compensate well for the influence of matched and mismatched external disturbances. Compared to the case without mismatched external disturbances, the tracking accuracy is maintained; the maximum tracking error is 2.386 [μm], and the positioning error is 0.0921 [μm]. This shows that the GESOISMC designed for the ball screw feed system has high immunity to the interferences existing in the system that both satisfy and dissatisfy the matching conditions.

4.2.3. Tracking Performance with Uncertainties

To verify the robustness of the designed controller to uncertainties of system parameters, the system parameters were set to be time-varying parameters during the tracking performance simulation as $k = 2.1153 \times 10^4 + 1.5 \times 10^4 \sin(4\pi t)$, $c = 2.6775 + 2\sin(4\pi t)$, and $m_1 = 0.6512 + 0.1\sin(4\pi t)$. The tracking error and control signal obtained are shown in Figure 11.
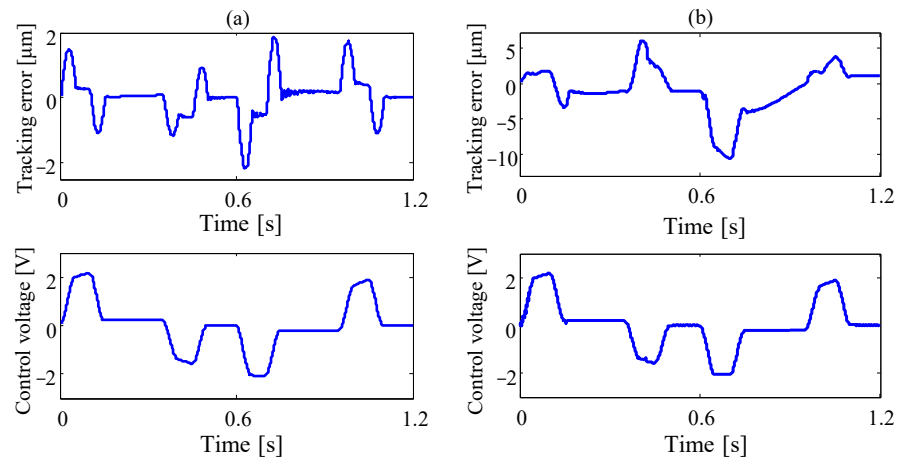

Figure 11. Simulation results of tracking performance with parameter uncertainties: (**a**) Case 1 and (**b**) Case 2.

As shown in Figure 11b, in the case of system uncertainties, the designed optimal guarantee coefficient matrix K_I has been optimized for system uncertainties. However, if the ISMC cannot fully compensate for the influence of the system parameter uncertainties, especially if the parameter uncertainties do not meet the matching conditions, the tracking error greatly increases, the maximum tracking error is 10.562 [μm], and the system uncertainties deform the tracking error curve. In contrast, the GESOISMC can compensate well for the effects of system uncertainties. The maximum tracking error is 2.166 [μm], and compared to the condition without system parameter uncertainties, the shape of the tracking error curve is maintained well, still showing the jerk curve of the reference trajectory. This shows that the GESOISMC designed for the ball screw feed system has strong robustness to system parameter uncertainties.

4.2.4. Tracking Performance with Vibration

When the frequency of external disturbances is close to the first-order axial vibration frequency of the system, the system resonance is excited. To verify the vibration suppression performance of the designed controller in the presence of vibration interference in the system, sinusoidal signals that satisfy and dissatisfy the matching conditions were added in the simulation process, whose frequency is near the natural frequency of the first-order vibration mode of the system, namely, $f_1 = 0.2\sin 190\pi t$[V] and $f_2 = 1.5\sin 190\pi t$[V]. The tracking error and control signal obtained from the simulation are shown in Figure 12.

As shown in Figure 12b, high-frequency sinusoidal interference signals excite the first-order axial vibration of the system, resulting in a great decline in tracking accuracy and dramatic fluctuations in tracking errors and control signals. The maximum tracking error of the ISMC is 8.206 [μm], while the fluctuation range of the constant-velocity stage reaches 13.38 [μm]. The GESOISMC with vibration compensation significantly improves the vibration suppression effect and the tracking accuracy of the system. The maximum tracking error is reduced to 2.488 [μm], and the fluctuation of the tracking error curve is also greatly reduced, while the fluctuation amplitude of the constant-velocity stage is reduced to 1.856 [μm]. In summary, the GESOISMC with vibration compensation designed for the flexible model of the system can effectively suppress the first-order axial vibration of the ball screw feed system and ensure the tracking accuracy of the system.
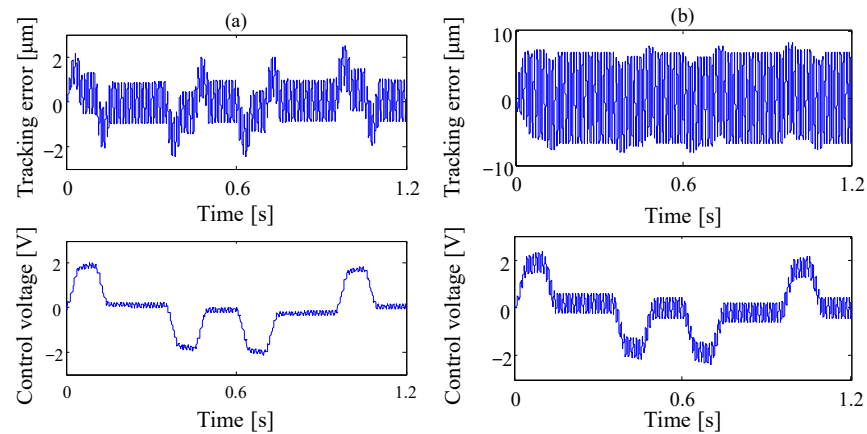
Figure 12. Simulation results of tracking performance with vibration interference. (**a**) Case 1; (**b**) Case 2.

4.3. Experimental Verification

To verify the comprehensive performance of the designed controller, the controller was applied to the high-speed ball screw feed experimental system shown in Figure 5 for tracking experiments. The tracking reference trajectory also uses the curve presented in Figure 8. After subdivision, the signal resolution of the rotary encoder is 0.04 [μm], and the signal separation rate of the linear grating ruler is 0.2 [μm]. During the process of the tracking experiment, the linear grating was used to feedback the displacement signal and speed signal of the table, and the rotary encoder was used to feedback the displacement signal and speed signal of the motor. The experimental comparison objects are the following: (1) Case 1: GESOISM with vibration compensation, and (2) Case 2: ISMC. To ensure the reliability of the experimental results, each test was repeated three times to obtain repeatable experimental results.

4.3.1. Tracking Performance

Firstly, the tracking performance of the designed controller was verified, and mass blocks and disturbance signals were not added during the experiment. The tracking error obtained from the experiment is shown in Figure 13. As illustrated in Figure 13a, the maximum tracking error of the ISMC is 25.96 [μm], and there is a tracking error much larger than that in the acceleration stage of the return journey, which may be caused by the friction of the linear guide rail, which is an external disturbance that dissatisfies the matching conditions. The RMS of the tracking error is 5.47 [μm], and there is a positioning error of 2.31 [μm]. In contrast, the maximum tracking error of the GESOISMC is reduced to 12.79 [μm], the RMS is reduced to 4.02 [μm], and the positioning error is reduced to 8.2×10^{-11} [μm]. This is because GESO compensates for the frictional interference and unmodeled dynamics present in the system.
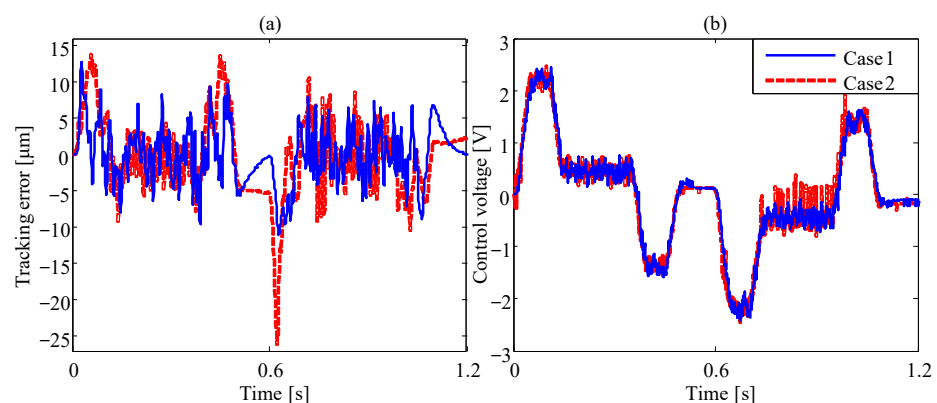

Figure 13. Tracking experimental results: (**a**) tracking error and (**b**) control signals.

4.3.2. Robustness Performance against System Uncertainties

To verify the robustness of the designed controller to the uncertainties of system parameters, 25 [kg] mass blocks were added to the table during the experiment. Adding the mass blocks could change the parameters of the system model. The tracking error obtained from the experiment is shown in Figure 14.
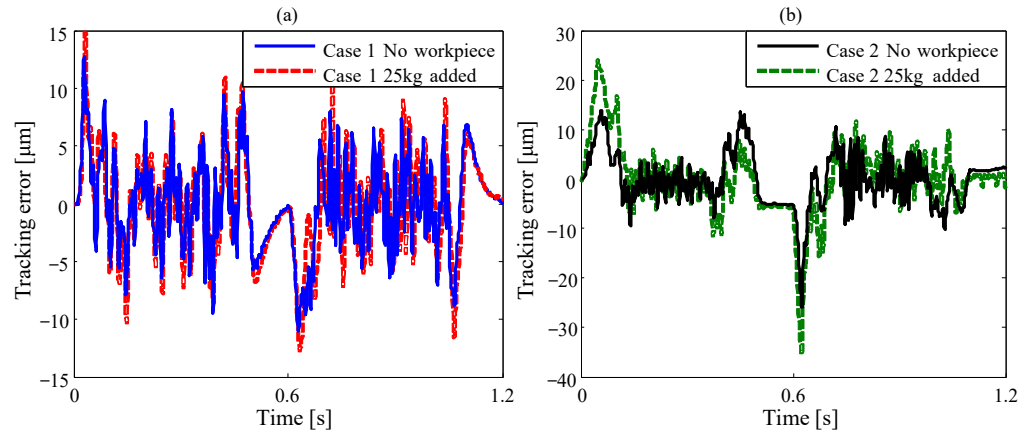

Figure 14. Comparison of tracking experimental results with no workpiece and with 25 [kg] workpiece added: (**a**) Case 1 and (**b**) Case 2.

As shown in Figure 14b, compared to the tracking error under the scenario without a workpiece, when a 25 [kg] workpiece is added, the tracking error of the ISMC increases significantly; the maximum tracking error is 35.51 [μm], and the RMS increases to 7.43 [μm]. In contrast, the GESOISMC maintains a tracking performance that is comparable to the scenario with no workpiece, with a maximum tracking error of 14.84 [μm] and an RMS of 4.45 [μm]. The results of the tracking experiment after adding the workpiece are consistent with the simulation results with increases in the parameter uncertainties, indicating that the GESOISMC designed for the ball screw feed system can compensate for the parameter uncertainties of the system more effectively.

4.3.3. Vibration Suppression Performance

To verify the tracking performance and vibration suppression performance of the designed controller in the presence of vibration interference in the system, a sinusoidal signal $f_1 = 1.2\sin190\pi t$[V] with a frequency near the first-order vibration frequency of the system was added to the voltage input signal. The tracking error obtained from the experiment is shown in Figure 15.
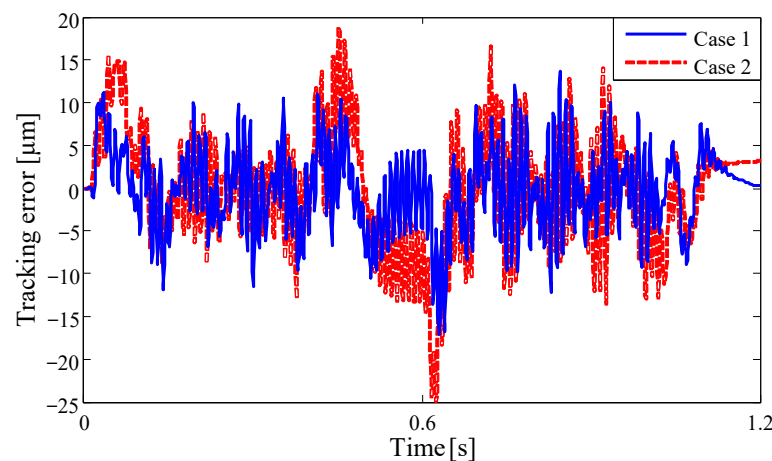

Figure 15. Tracking experimental results with vibration interference.

By comparing the tracking error of the two controllers, it can be seen that the tracking error of the ISMC fluctuates greatly when there is vibration interference in the system. The maximum tracking error decreases to 24.93 [μm], but the RMS increases to 6.831 [μm], and the positioning error increases to 3.28 [μm]. The GESOISMC + vibration compensation has better vibration suppression performance than the ISMC. The fluctuation of the tracking error is significantly smaller than that of the ISMC, with the maximum tracking error equal to 15.98 [μm], indicating a slight increase, the RMS increases to 4.86 [μm], and the positioning error increases to 0.25 [μm]. Additionally, the overall vibration suppression effect is better than the ISMC. After adding vibration interference, the tracking experimental results are consistent with the simulation results. The GESOISMC + vibration compensation designed for the flexible ball screw feed system can effectively suppress the first-order axial vibration of the system and ensure the tracking accuracy of the system.

The experimental data of the tracking experiment are summarized in Table 2, which can more directly reflect the performance of different controllers.

Table 2. Summary of tracking experimental data.

	Case	Maximum Absolute Value of Tracking Error [μm]	RMS [μm]	Positioning Error [μm]
No workpiece	1	12.79	4.02	8.2×10^{-11}
	2	25.96	5.47	2.31
Addition of 25 kg workpiece	1	14.84	4.45	0.42
	2	35.51	7.43	1.25
Vibration interference	1	15.98	4.86	0.25
	2	24.93	6.831	3.28

5. Conclusions

In this paper, an integral sliding mode controller based on a generalized extended state observer is proposed for the flexible body model of a ball screw feed system, and vibration compensation is designed. The purpose of this method is to effectively compensate for system perturbations that satisfy and dissatisfy the matching conditions of the ball screw feed system and to further suppress first-order axial vibration induced by system disturbances. The simulation and experimental results show that the designed GESOISMC with vibration compensation has several advantages: Firstly, the addition of GESO effectively solves the defect that an ordinary ISMC cannot compensate for mismatched perturbations and significantly improves the anti-interference performance of the controller. Secondly, the GESOISMC with vibration compensation is more robust to parameter uncertainties and first-order axial vibration of the ball screw feed system, resulting in better tracking performance. In conclusion, the developed control method is expected to provide better dynamic performance for ball screw feed drives.

Author Contributions: Conceptualization, M.Z.; methodology, M.Z. and D.B.; software, M.Z.; validation, M.Z., D.B. and X.H.; formal analysis, M.Z.; writing—original draft preparation, M.Z.; writing—review and editing, M.Z. and X.H.; funding acquisition, M.Z. All authors have read and agreed to the published version of the manuscript.

Data Availability Statement: Data sharing is not applicable to this article.

Conflicts of Interest: The authors declare no conflict of interest.

References

1. Masih, H. Linear Parameter-Varying Control of CNC Machine Tool Feed-Drives with Dynamic Variations. Master's Thesis, University of British Columbia, Vancouver, Canada, 2014.

2. Altintas, Y.; Verl, A.; Brecher, C.; Uriarte, L.; Pritschow, G. Machine tool feed drives. *CIRP Ann. Manuf. Technol.* **2011**, *60*, 779–796. [CrossRef]

3. Sepasi, D. Modeling of linear systems with parameter variations: Applications in hard disk and ball screw drives. Master's Thesis, University of British Columbia, Vancouver, Canada, 2011.

4. Pritschow, G. On the influence of the velocity gain factor on the path deviation. *CIRP Annals Manuf. Technol.* **1996**, *45*, 367–371. [CrossRef]

5. Cho, J.U.; Le, Q.N.; Jeon, J.W. An FPGA-based multiple-axis motion control chip. *IEEE Trans. Ind. Electron.* **2009**, *56*, 856–870.

6. Wai, R.J.; Lee, J.D.; Chuang, K.L. Real-time pid control strategy for maglev transportation system via particle swarm optimization. *IEEE Trans. Ind. Electron.* **2011**, *58*, 629–646. [CrossRef]

7. Erkorkmaz, K.; Kamalzadeh, A. High bandwidth control of ball screw drives. *CIRP Ann.-Manuf. Technol.* **2006**, *55*, 393–398. [CrossRef]

8. Yao, B.; Al-Majed, M.; Tomizuka, M. High-performance robust motion control of machine tools: An adaptive robust control approach and comparative experiments. *IEEE/ASME Trans. Mechatron.* **2002**, *2*, 63–76.

9. Boucher, P.; Dumur, D.; Rodriguez, P. Robustification of CNC Controllers for Machine Tools Motor Drives. *CIRP Ann. Manuf. Technol.* **2003**, *52*, 293–296. [CrossRef]

10. Nguyen, D.G.; Tran, D.T.; Ahn, K.K. Disturbance observer-based chattering-attenuated terminal sliding mode control for nonlinear systems subject to matched and mismatched disturbances. *Appl. Sci.* **2021**, *11*, 8158. [CrossRef]

11. Bhaskarwar, T.; Hawari, H.F.; Nor, N.B.M.; Chile, R.H.; Waghmare, D.; Aole, S. Sliding Mode Controller with Generalized Extended State Observer for Single Link Flexible Manipulator. *Appl. Sci.* **2022**, *12*, 3079. [CrossRef]

12. Kamalzadeh, A.; Erkorkmaz, K. Compensation of axial vibrations in ball screw drives. *CIRP Ann. Manuf. Technol.* **2007**, *56*, 373–378. [CrossRef]

13. Okwudire, C.; Altintas, Y. Minimum tracking error control of flexible ball screw drives using a discrete-time sliding mode controller. *J. Dyn. Syst. Meas. Control.* **2009**, *131*, 051006. [CrossRef]

14. Jamaludin, Z.; Van Brussel, H.; Swevers, J. Quadrant glitch compensation using friction model-based feedforward and an inverse-model-based disturbance observer. In Proceedings of the 2008 10th IEEE International Workshop on Advanced Motion Control, Trento, Italy, 26–28 March 2008; pp. 212–217.

15. Dong, L.; Tang, W.C. Adaptive backstepping sliding mode control of flexible ball screw drives with time-varying parametric uncertainties and disturbances. *ISA Trans.* **2014**, *53*, 110–116. [CrossRef]

16. Gordon, D.J.; Erkorkmaz, K. Accurate control of ball screw drives using pole-placement vibration damping and a novel trajectory prefilter. *Precis. Eng.* **2013**, *7*, 308–322. [CrossRef]

17. Altintas, Y.; Khoshdarregi, M.R. Contour error control of CNC machine tools with vibration avoidance. *CIRP Ann. Manuf. Technol.* **2012**, *61*, 335–338. [CrossRef]

18. Fujimoto, H.; Takemura, T. High-precision control of ball-screw-driven stage based on repetitive control using n-times learning filter. *IEEE Trans. Ind. Electron.* **2014**, *61*, 3694–3703. [CrossRef]

19. Tsai, M.S.; Yen, C.L.; Yau, H.T. Integration of an empirical mode decomposition algorithm with iterative learning control for high-precision machining. *IEEE/ASME Trans. Mechatron.* **2013**, *18*, 878–886. [CrossRef]

20. Zhang, C.; Chen, Y. Tracking control of ball screw drives using ADRC and equivalent-error-model-based feedforward control. *IEEE Trans. Ind. Electron.* **2016**, *63*, 7682–7692. [CrossRef]

21. Rajabi, N.; Abolmasoumi, A.H.; Soleymani, M. Sliding mode trajectory tracking control of a ball-screw-driven shake table based on online state estimations using EKF/UKF. *Struct. Control. Health Monit.* **2018**, *25*, e2133. [CrossRef]

22. Park, S.C.; Lee, J.M.; Han, S.I. Tracking error constrained terminal sliding mode control for ball-screw driven motion systems with state observer. *Int. J. Precis. Eng. Manuf.* **2018**, *19*, 359–366. [CrossRef]

23. Sun, Z.; Pritschow, G.; Zahn, P. A novel cascade control principle for feed drives of machine tools. *CIRP Ann.* **2018**, *67*, 389–392. [CrossRef]

24. Simba, K.R.; Bui, B.D.; Msukwa, M.R.; Uchiyama, N. Robust iterative learning contouring controller with disturbance observer for machine tool feed drives. *ISA Trans.* **2018**, *75*, 207–215. [CrossRef] [PubMed]

25. Li, F.; Jiang, Y.; Li, T.; Ehmann, K.F. Compensation of dynamic mechanical tracking errors in ball screw drives. *Mechatronics* **2018**, *55*, 27–37. [CrossRef]

26. Hayashi, T.; Fujimoto, H.; Isaoka, Y. Projection-based iterative learning control for ball-screw-driven stage with consideration of rolling friction compensation. *IEEJ J. Ind. Appl.* **2020**, *9*, 132–139. [CrossRef]

27. Hayashi, T.; Fujimoto, H.; Isaoka, Y. Negative quadrant glitch suppression control of ball-screw-driven stage for machine tool by friction compensation and initial value compensation. *Electr. Eng. Jpn.* **2022**, *215*, e23402. [CrossRef]

28. Sencer, B.; Dumanli, A. Optimal control of flexible drives with load side feedback. *CIRP Ann.* **2017**, *66*, 357–360. [CrossRef]

29. Dumanli, A.; Sencer, B. Optimal high-bandwidth control of ball-screw drives with acceleration and jerk feedback. *Precis. Eng.* **2018**, *54*, 254–268. [CrossRef]

30. Yang, M.; Ni, Q.; Liu, X. Vibration suppression and over-quadrant error mitigation methods for a ball-screw driven servo system with dual-position feedback. *IEEE Access* **2020**, *8*, 213758–213771. [CrossRef]

31. Shirvani, H.K.; Hosseinkhani, Y.; Erkorkmaz, K. Suppression of harmonic positioning errors in ball-screw drives using Adaptive Feedforward Cancellation. *Precis. Eng.* **2021**, *68*, 235–255. [CrossRef]

32. Huang, C.-L.; Wang, T.; Li, M.; Yu, Y. Sliding Mode Control of Servo Feed System Based on Fuzzy Reaching Law. *Appl. Sci.* **2023**, *13*, 6086. [CrossRef]

33. Dong, L.; Tang, W.C.; Bao, D.F. Interpolating gain-scheduled H∞ loop shaping design for high speed ball screw feed drives. *ISA Trans.* **2015**, *55*, 219–226. [CrossRef]

34. Hanifzadegan, M.; Nagamune, R. Tracking and structural vibration control of flexible ball–screw drives with dynamic variations. *IEEE/ASME Trans. Mechatron.* **2015**, *20*, 133–142. [CrossRef]

35. Zhang, L.; Liu, J.; Zhuang, C. Gain scheduling control of ball screw feed drives based on linear parameter varying model. *Int. J. Adv. Manuf. Technol.* **2022**, *11–12*, 4493–4510. [CrossRef]

36. Siddiqui, M.A.; Anwar, M.N.; Laskar, S.H. Tuning of PIDF controller in parallel control structure for integrating process with time delay and inverse response characteristic. *J. Control. Autom. Electr. Syst.* **2020**, *31*, 829–841. [CrossRef]

37. Liu, C.; Zhao, C.; Liu, Z.; Wang, S. Dynamic Analysis of Ball Screw Feed System with the Effects of Excitation Amplitude and Design Parameters. *Appl. Sci.* **2021**, *11*, 7070. [CrossRef]

38. Utkin, V.; Shi, J. Integral sliding mode in systems operating under uncertainty conditions. In Proceedings of the 35th IEEE Conference on Decision and Control, Kobe, Japan, 13 December 1996; pp. 4591–4596.

39. Bejarano, F.J.; Fridman, L.M.; Poznyak, A.S. Output integral sliding mode for min-max optimization of multi-plant linear uncertain systems. *IEEE Trans. Autom. Control.* **2009**, *54*, 2611–2620. [CrossRef]

40. Hamayun, M.T.; Edwards, C.; Alwi, H. *Fault Tolerant Control Schemes Using Integral Sliding Modes*; Springer International Publishing: Cham, Switzerland, 2016; pp. 17–36.

41. Li, H.; Shi, P.; Yao, D. Observer-based adaptive sliding mode control for nonlinear Markovian jump systems. *Automatica* **2016**, *64*, 133–142. [CrossRef]

42. Li, S.; Yang, J.; Chen, W.-H.; Chen, X. Generalized extended state observer based control for systems with mismatched uncertainties. *IEEE Trans. Ind. Electron.* **2011**, *59*, 4792–4802. [CrossRef]

43. Gao, Z. Active disturbance rejection control: A paradigm shift in feedback control system design. In Proceedings of the American Control Conference, Minneapolis, MN, USA, 14–16 June 2006; pp. 2399–2405.